

Laser-plasma electron accelerator for all optical inverse-Compton x-ray source

K. Koyama
University of Tokyo

A. Maekawa, A. Yamazaki, and M. Uesaka
University of Tokyo

T. Hosokai

Tokyo Institute of Technology

M. Miyashita

Tokyo University of Science

S. Masuda and E. Miura

National Institute of Advanced Industrial Science and Technology (AIST)

OUTLINE

- ALL OPTICAL INVERSE-COMPTON X-RAY SOURCES

- LASER-PLASMA ELECTRON ACCELERATORS

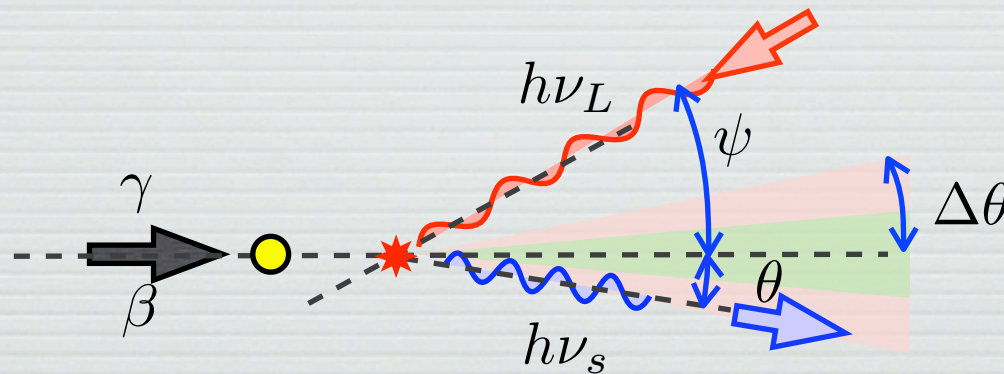
(WAKEFIELD ACCELERATORS)

PRINCIPLE AND CHARACTERISTICS

- STABILIZATION OF WAKE-FIELD ACCELERATORS

Inverse Compton x-ray source

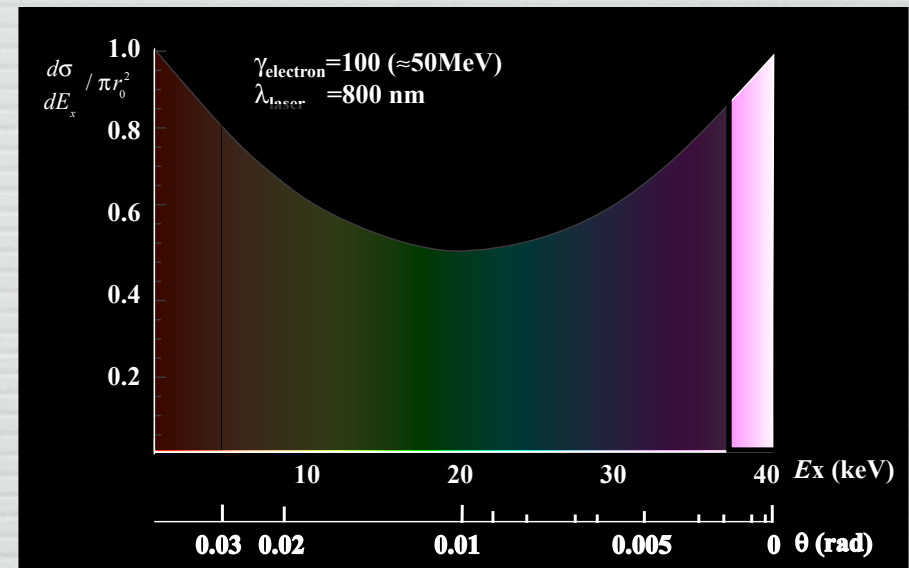
Inverse Compton scattering provides a monochromatic x-ray pulse by Doppler upshifting of an intense laser pulse.



$$h\nu_s \simeq h\nu_L \frac{2\gamma^2 (1 + \beta \cos \psi)}{1 + (\gamma\theta)^2}$$

$$h\nu \ll mc^2, \quad \theta \ll 1, \quad a_0 \ll 1$$

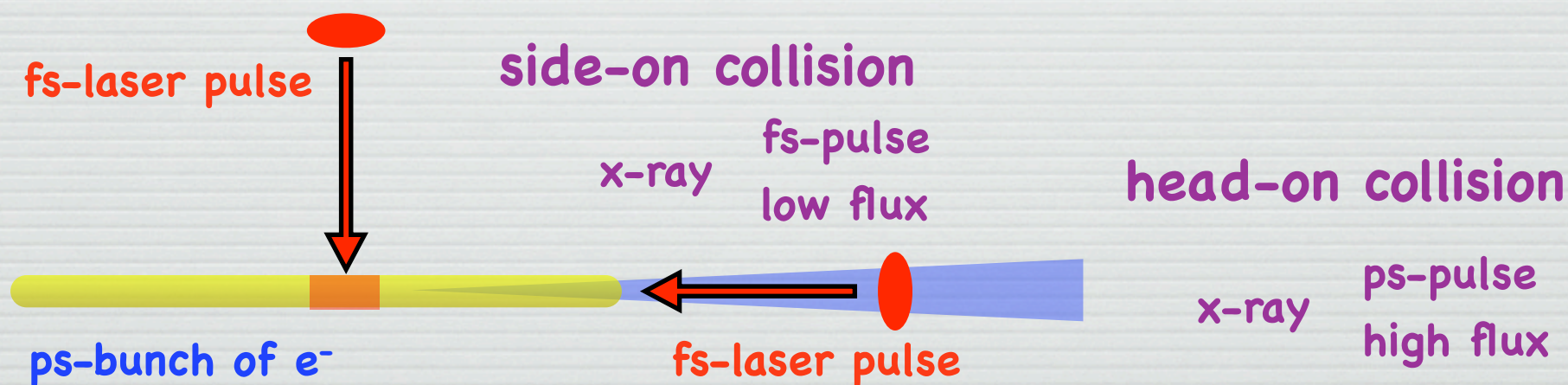
$$\Delta\theta = 1/\gamma$$



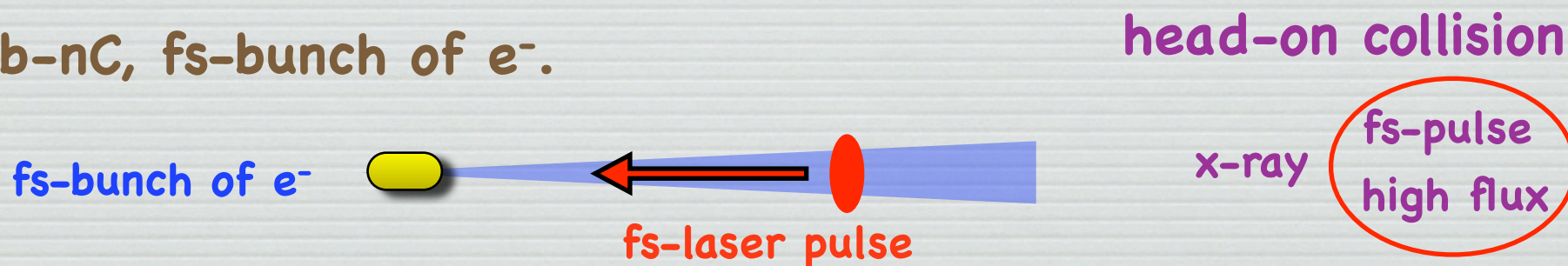
Inverse Compton x-ray source II

Duration of x-ray pulse $\propto e^-$ -bunch length + laser pulse

Intensity of x-ray pulse \propto number of interaction $e^- \times h\nu$ -density



Laser wakefield accelerator can deliver a sub-nC, fs-bunch of e^- .



Inverse Compton x-ray source III

$\approx 10^7$ X-ray photons per shot

$\approx 100\text{pC}, 10^{17} \text{ W/cm}^2, 5 \times 10^{-9} \text{ cm}^3$

to produce a few-MeV photons (@ 1eV)

$$h\nu_s \simeq 4\gamma^2 \cdot h\nu_L, \quad (\psi \approx 0, \theta \approx 0) \quad 0.4 \sim 0.5 \text{ GeV}$$

	Accel. gradient	Length for 500MeV
rf-linac	10-40 MeV/m	$\approx 25 \sim 50 \text{ m}$
LWFA	96 GeV/m	$\approx 5 \text{ mm}$

Laser wakefield electron accelerator

1. Electrons are expelled by the laser pulse.

ponderomotive force

$$\mathbf{f}_{NL} = -\frac{e^2}{4m\omega^2} \nabla E_s^2$$

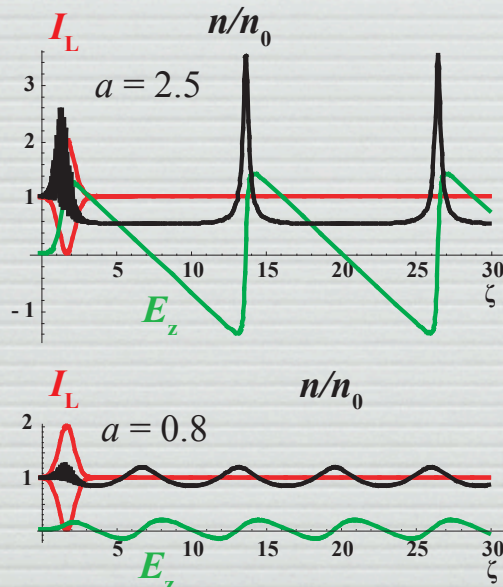
2. Displaced electrons are pulled back by the Coulomb force.

plasma wave is excited behind the laser pulse (wakefield)

traveling at the speed of light

$$\left(\frac{\partial^2}{\partial t^2} + \omega_{pe}^2 \right) \phi = \frac{mc^2}{4e} \omega_{pe}^2 a^2$$

3. Electrons riding the wakefield are accelerated.



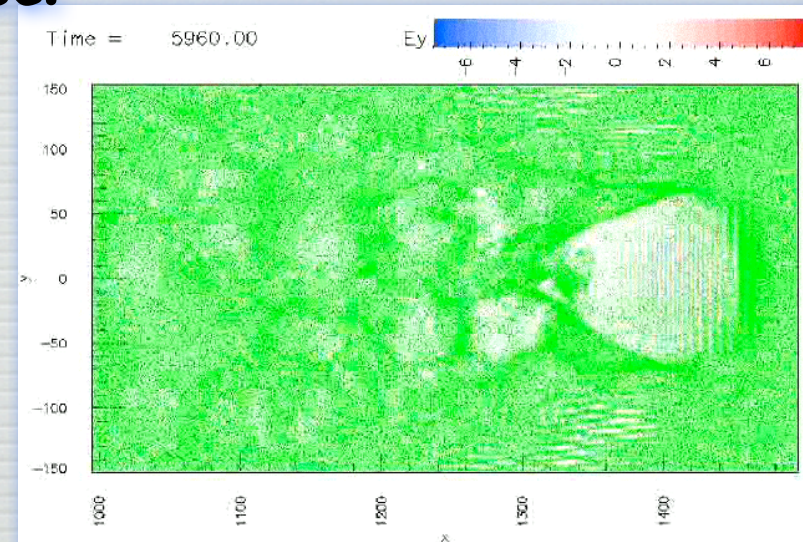
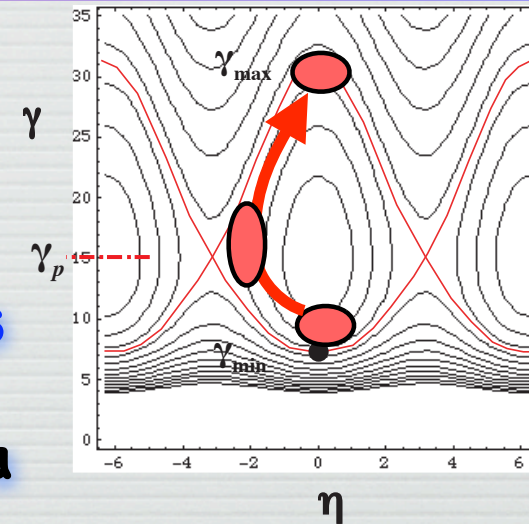
$$E_{WB}/E_0 = [2(\gamma_{ph} - 1)]^{1/2}$$

$$E_0 = cm\omega_{pe}/e$$

$$E_0 = 96 \text{ GV/m for } n_e = 10^{18} \text{ cm}^{-3}$$

Mono-energetic electron acceleration

1. Electrons should be accelerated by a single well.
 - ▶ excitation of single well
 - ▶ electron injection to one of wells
2. Initial electrons must be injected in a small portion of the phase space.
 - ▶ self-trapping
 - ▶ external injection
3. Acceleration length
 \approx dephasing length

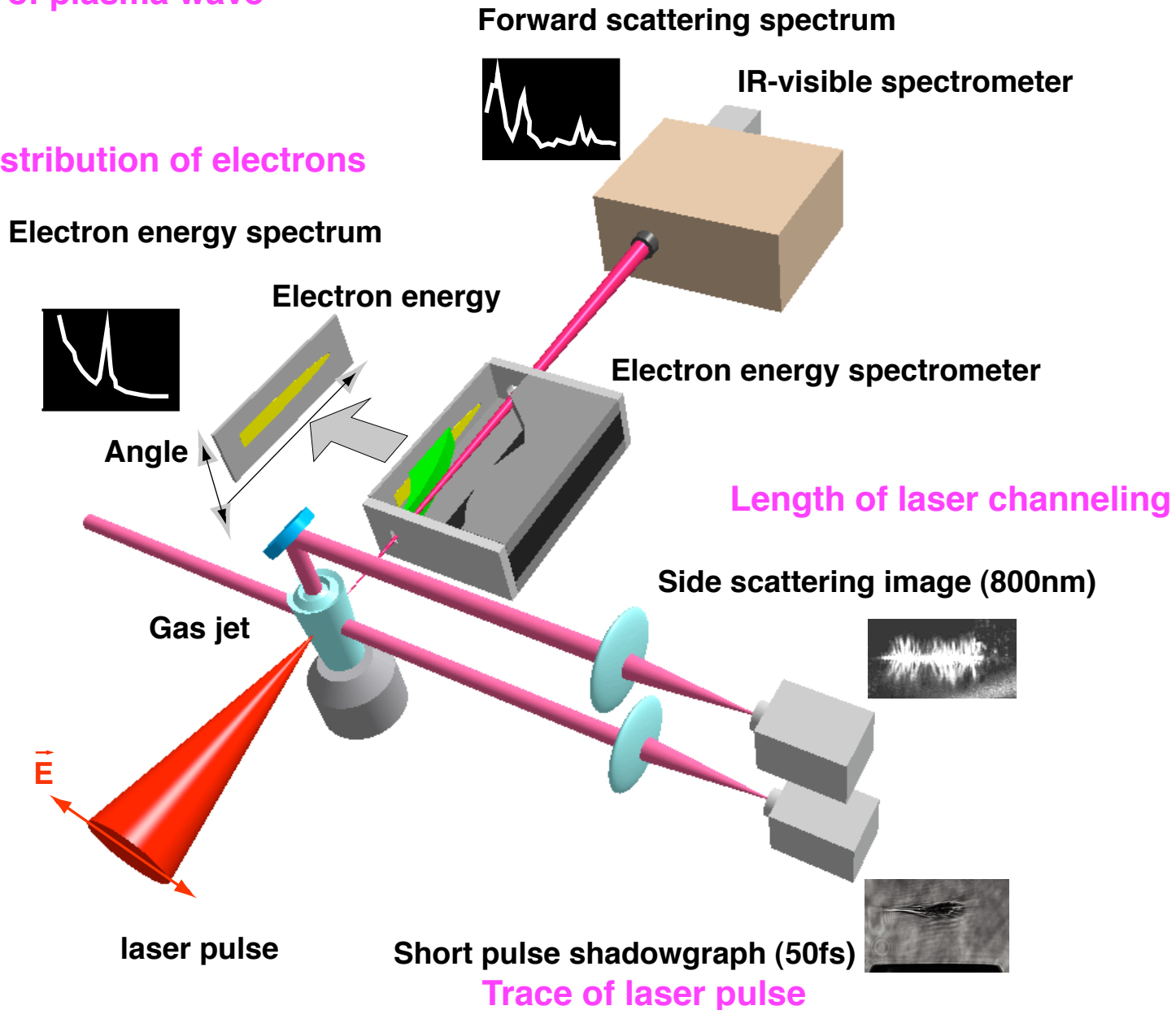


Schematic drawing of experimental setup



Amplitude of plasma wave

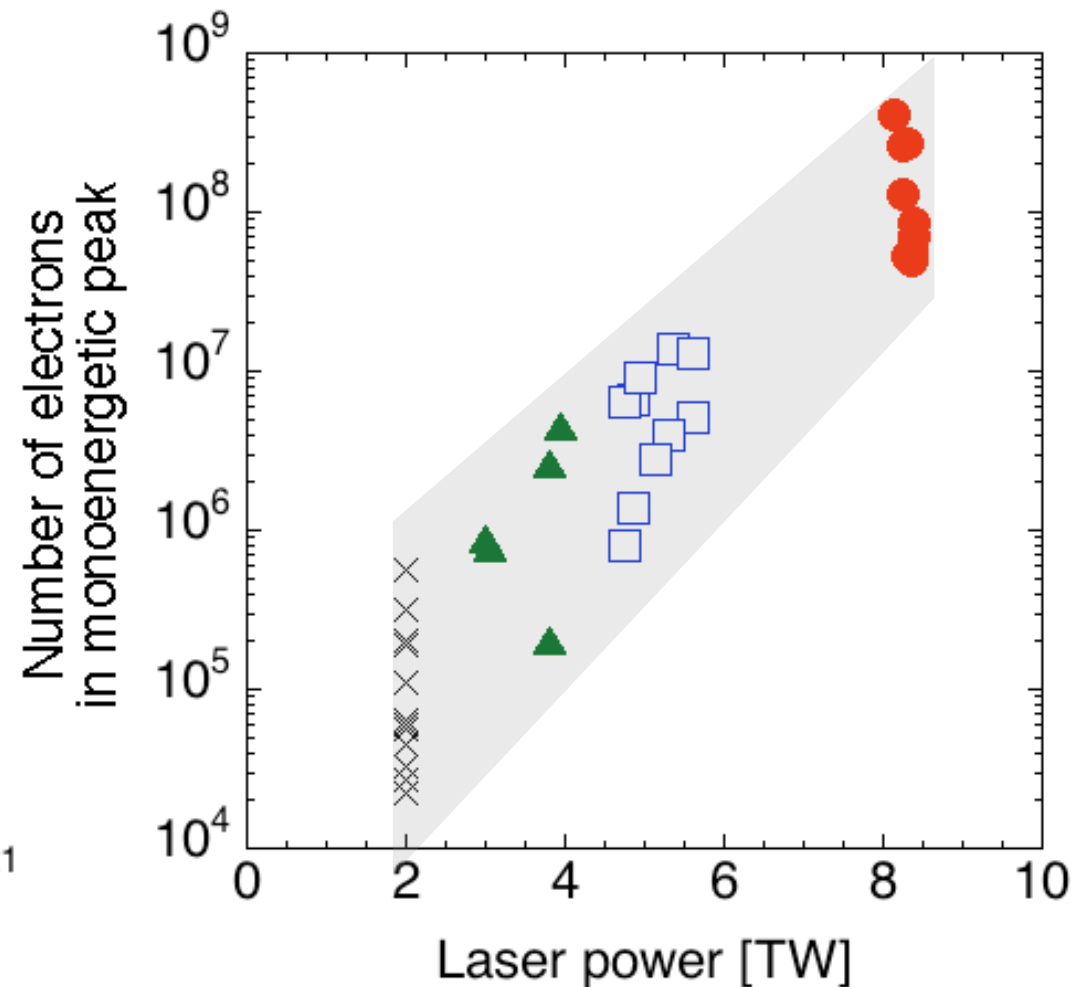
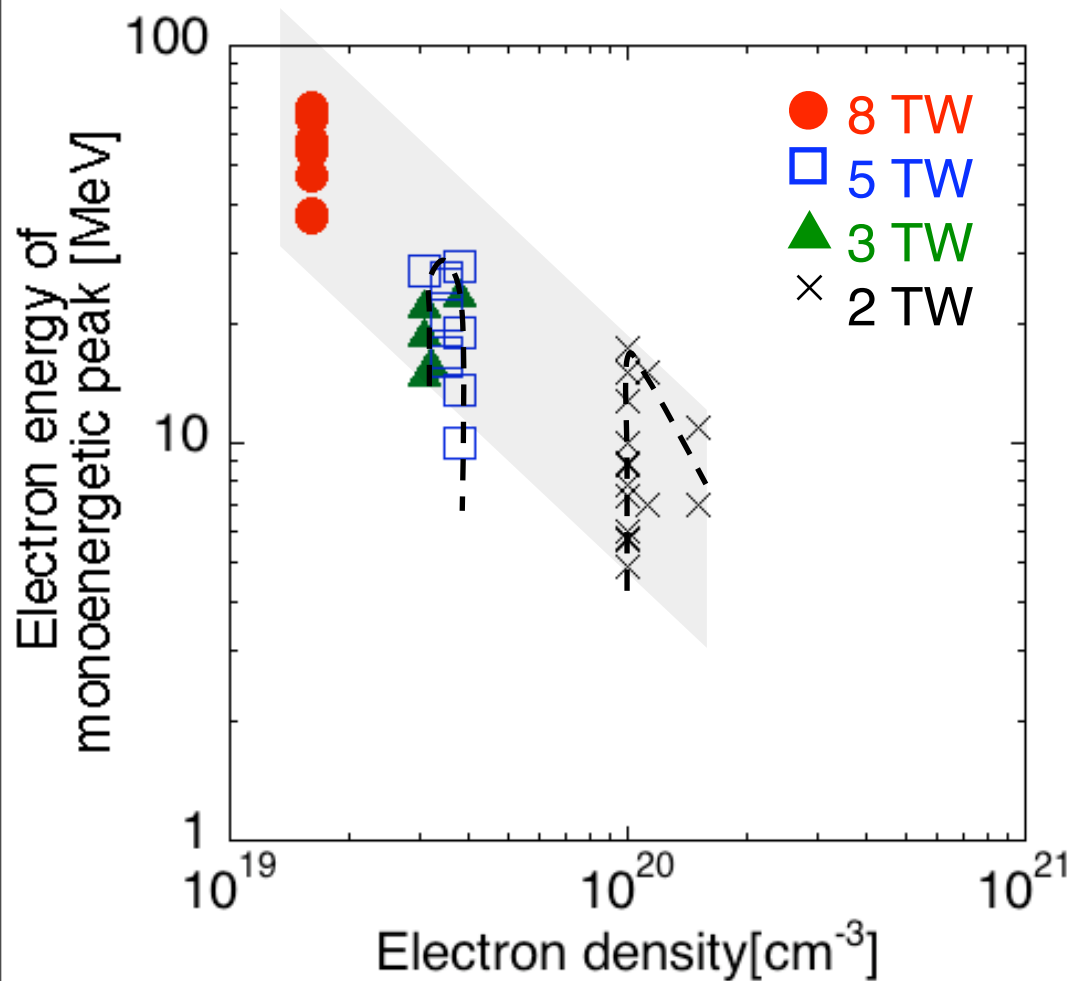
Energy-distribution of electrons



Recent activities of LWFA experiments at AIST and U.Tokyo

- ☒ Empirical scaling law of LWFA.
- ☒ Electron injection at a density step.
 - density jump formation by the shock wave
- ☒ Axial magnetic to stabilize LWFA.
 - deep capillary formation by the expanding shock in B-field
 - electron injection and post acceleration
 - ≈ 0.5 GeV by 8 TW laser pulse

Scaling and achieved parameters in quasi-monoenergetic electron beam generation



(by courtesy of E. Miura, AIST)

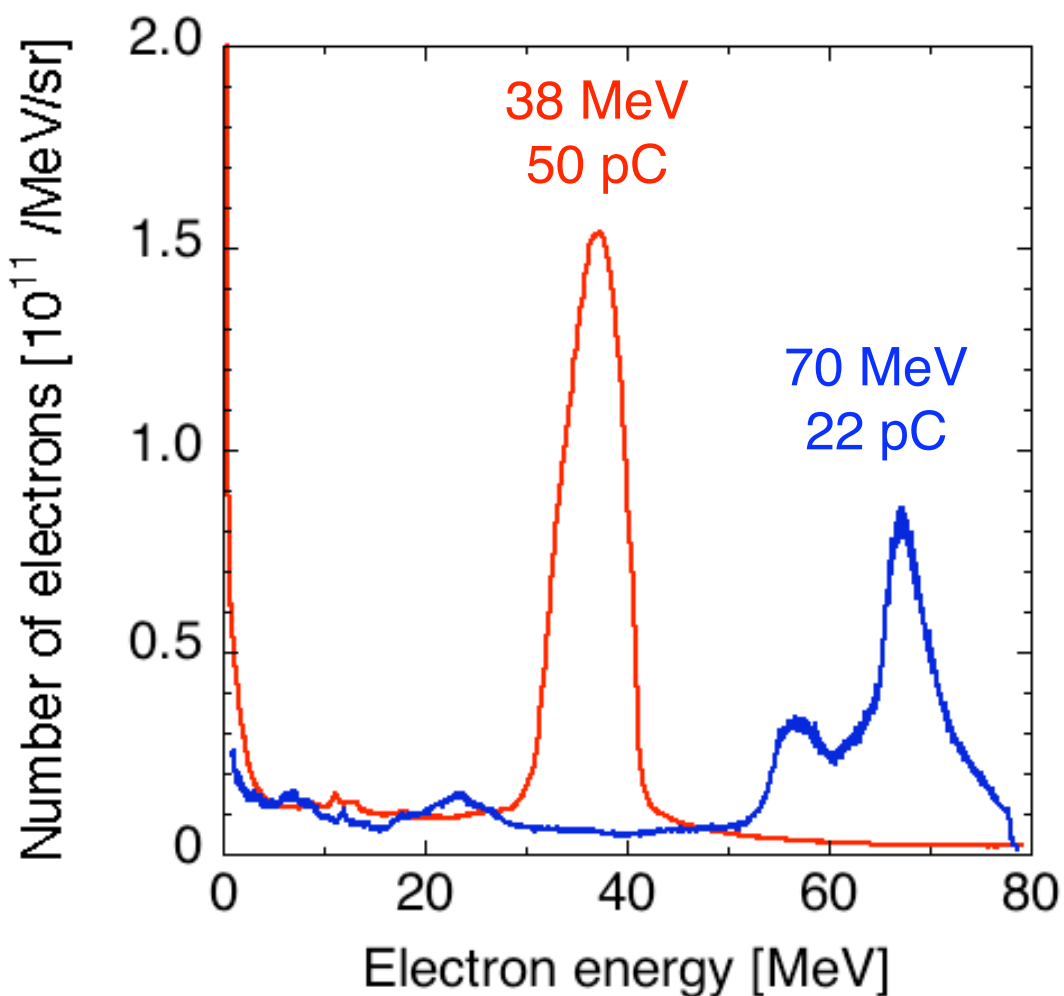
Stable generation of quasi-monoenergetic electron beam by self-injection scheme



Laser : 8.5 TW / 50 fs

Electron density : $1.6 \times 10^{19} \text{ cm}^{-3}$

Statistics of quasi-monoenergetic beams in consecutive 20 shots



Parameters	Mean (\pm s.d.)
Peak energy	$55 \pm 16 \text{ MeV}$
Energy spread ($\Delta E_{\text{FWHM}}/E$)	$21 \pm 11 \%$
Charge in peak	$15 \pm 10 \text{ pC}$
Beam divergence (FWHM)	$7.6 \pm 3.5 \text{ mrad}$
Beam pointing	$\pm 7.6 \text{ mrad}$
Probability of generation	80%

(by courtesy of E. Miura, AIST)

For increasing stability

Energy

Energy width

Electronic charge

Emittance

Beam pointing

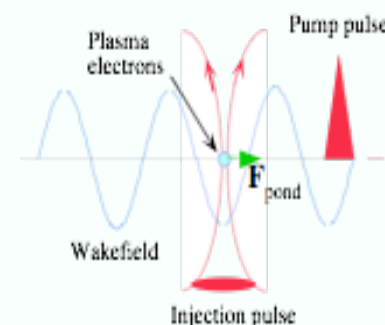
- ☒ Amplitude of the wakefield
- ☒ External injection of initial electrons
- ☒ Acceleration-length
- ☒ Laser guiding

Electron injections

Locally increased ponderomotive force produced by colliding laser pulses

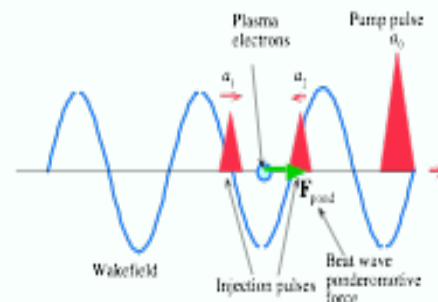
The laser pulse crosses the wakefield

D.Umstadter *et al.*, Phys. Rev. Lett. **76**, 2073 (1996).



Beatwave injection

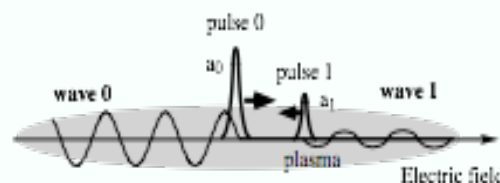
E. Esarey *et al.*, Phys. Rev. Lett. **79**, 2683 (1997).



Standing wave

H. Kotaki *et al.*, Phys. Plasmas **11**, 3296 (2004).

J. Faure *et al.*, Nature **444**, 737 (2006).

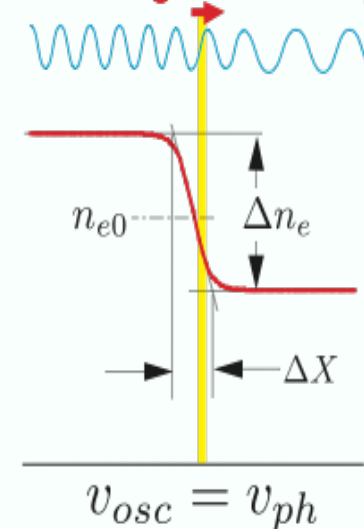


Local wavebreaking at the density ramp

S. V. Bulanov, Plasma Phys. Rep. **25**, 468 (1999).

T. Hosokai *et al.*, Phys. Rev.E **67**, 036407 (2003).

Wavebreaking / Electron injection



Wavebreaking at the density ramp

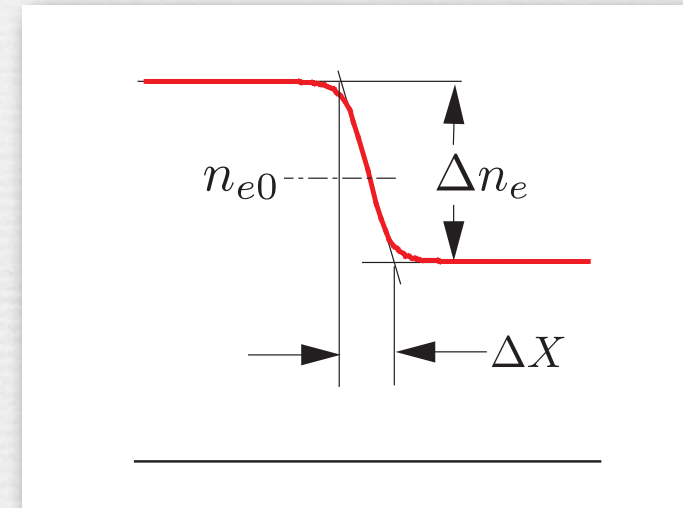
- The local wave number of the plasma wave, which propagate from high-density to low-density, i.e. from large ω_{pe} to small ω_{pe} , increases in time.

$$\frac{\partial}{\partial t} k_{pe}(t, z) = -\frac{\partial}{\partial z} \omega_{pe}(t, z)$$

- The phase velocity of the plasma wave $v_{ph} = \omega_{pe}/k_{pe}$ decreases.
- When the phase velocity is equal to the quivering velocity of the plasma wave v_q , the portion of the wave breaks.

$$v_q = \xi_m \omega_{pe} \sin(k_{pe} z_0 - \omega_{pe} t)$$

$$k_{pe} \xi_m = 1 \quad (v_{ph} = v_q)$$



The wave breaking occurs at the density discontinuity of the plasma.

The density of injected electron.
$$n_{inj} \approx n_{e0} \frac{\xi_m}{\Delta X} = n_{e0} \frac{1}{k \Delta X}$$

S. Bulanov, *et al.*, Phys. Rev. E **58**, R5257 (1998).

P. Tomassini, *et al.*, Phys. Rev. STAB **6**, 121301 (2003).

Methods for producing density ramps in plasmas

Shock front of the laser heated cavity

T.Hosokai, *et al.*, Phys. Rev. E **67**, 036407 (2003)

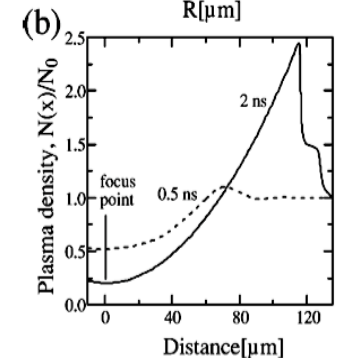
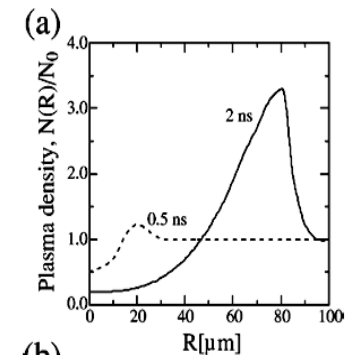
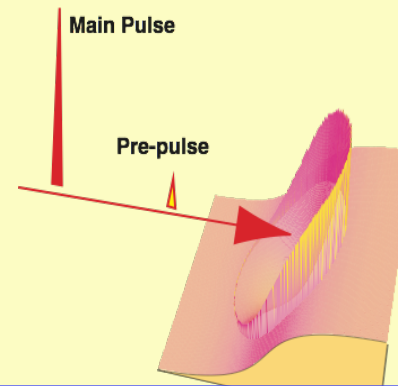
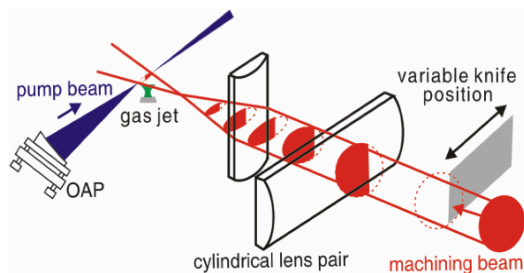


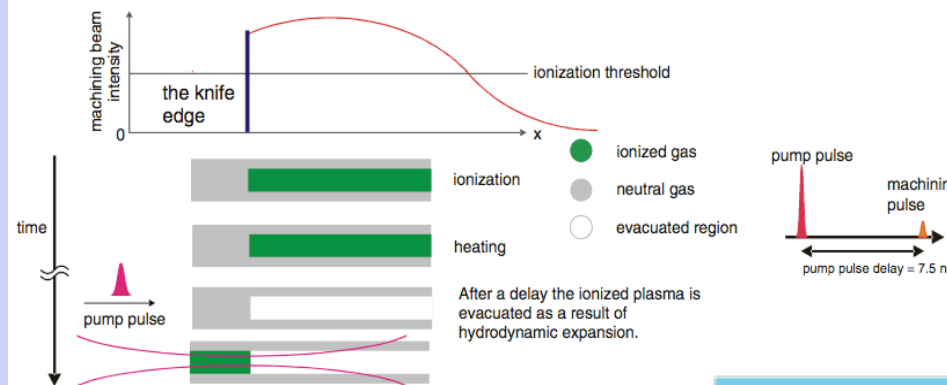
FIG. 6. Density distributions of a He jet after the laser prepulse calculated by 2D hydrodynamic simulation. The power density of the prepulse is $10^{13} \text{ W cm}^{-2}$ and the Rayleigh length is $50 \mu\text{m}$. (a) Radial direction ($x=0$), (b) longitudinal direction ($r=0$).

Laser machining of the plasma



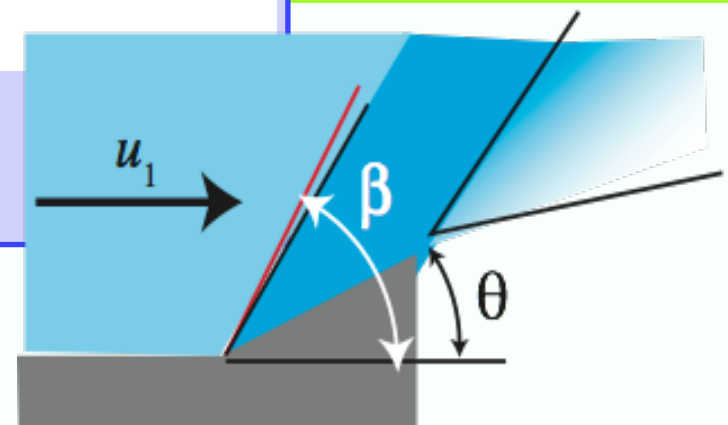
laser parameters:

	pump beam	machining beam
energy	230 mJ	60 mJ
pulse duration (FWHM)	45 fs	45 fs
beam size	40 mm	40 mm
focal spot (FWHM)	10 μm	20 μm x 1.3 mm



C.-T. Hsieh, *et al.*, Physical Review Letters **96**, 095001 (2006)

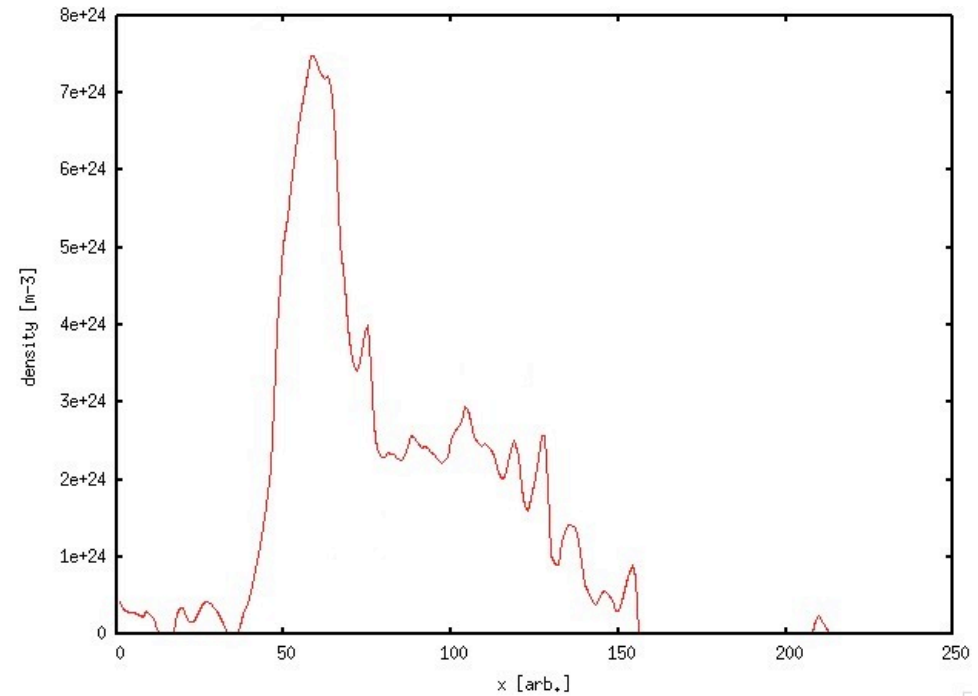
Oblique shock wave in a supersonic flow



Density ramp formed by the oblique shock

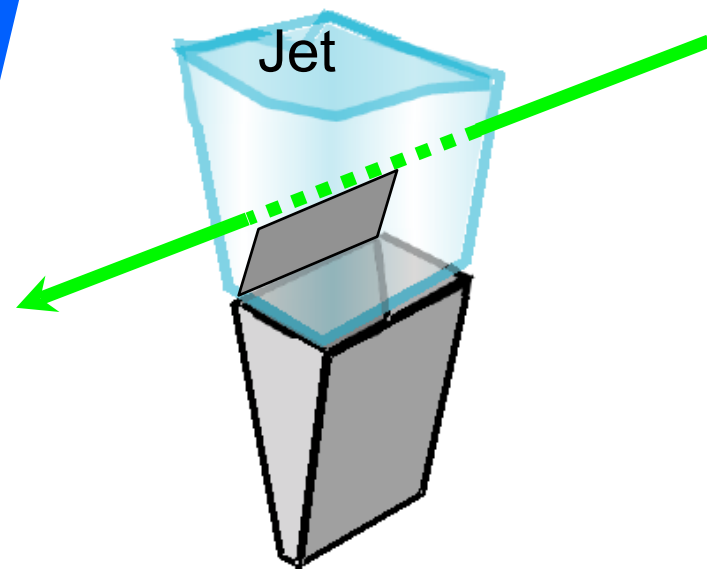
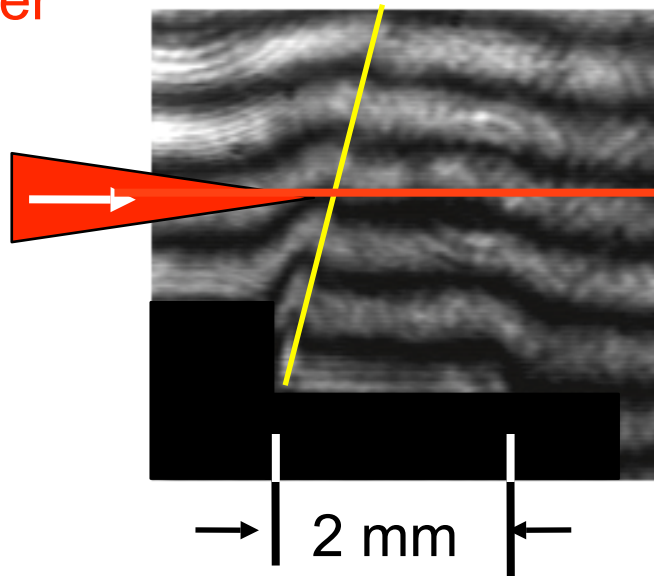
The density ramp was produced by the oblique shock.

$$n_2/n_1 \approx 3, L_n \ll 100 \mu\text{m}, n_1 \approx 10^{19} \text{ cm}^{-3}$$



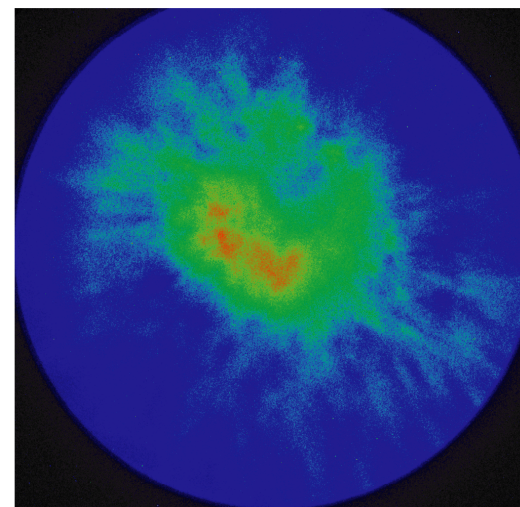
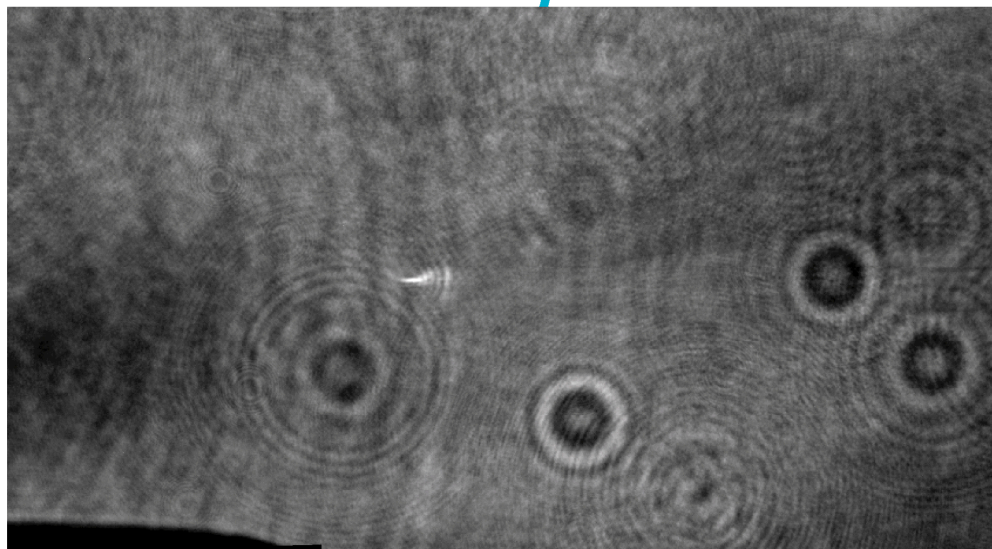
TW-laser
pulse

Oblique shock

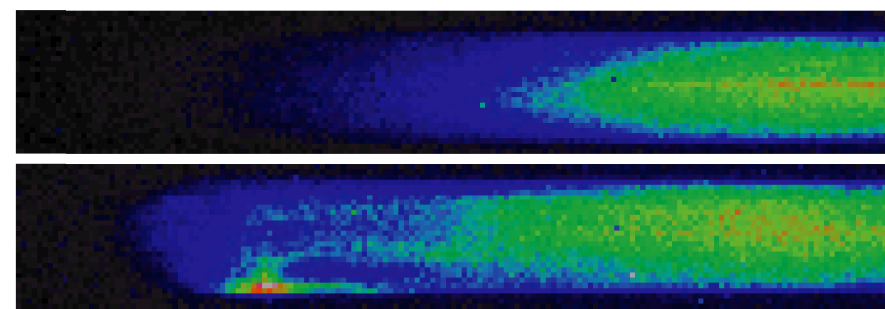


Preliminary result

Shock wave



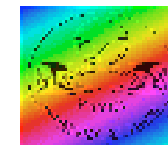
Gas flow



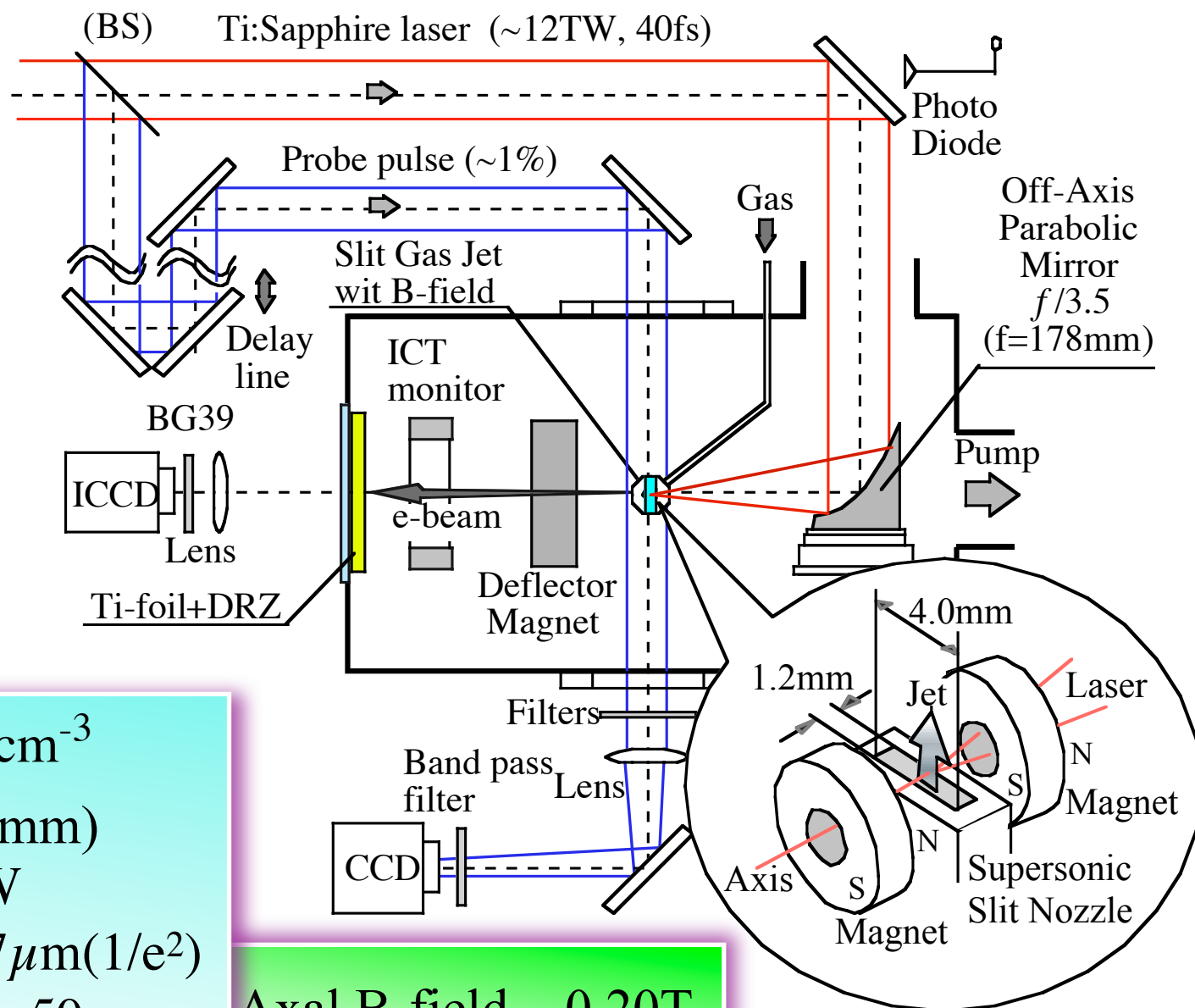
80 40 (MeV) 20



Repeatable LWFA with external B-field



T.Hosokai, et al., Phys Rev.Lett. 97, 075004 (2006)



He Gas $\sim 4 \times 10^{19} \text{ cm}^{-3}$

$F^\# = 3.5$ ($f = 178 \text{ mm}$)

Laser 6 ~ 12 TW

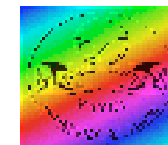
Focal spot $\sim 5\text{-}7 \mu\text{m}$ ($1/e^2$)

Rayleigh length $\sim 50 \mu\text{m}$

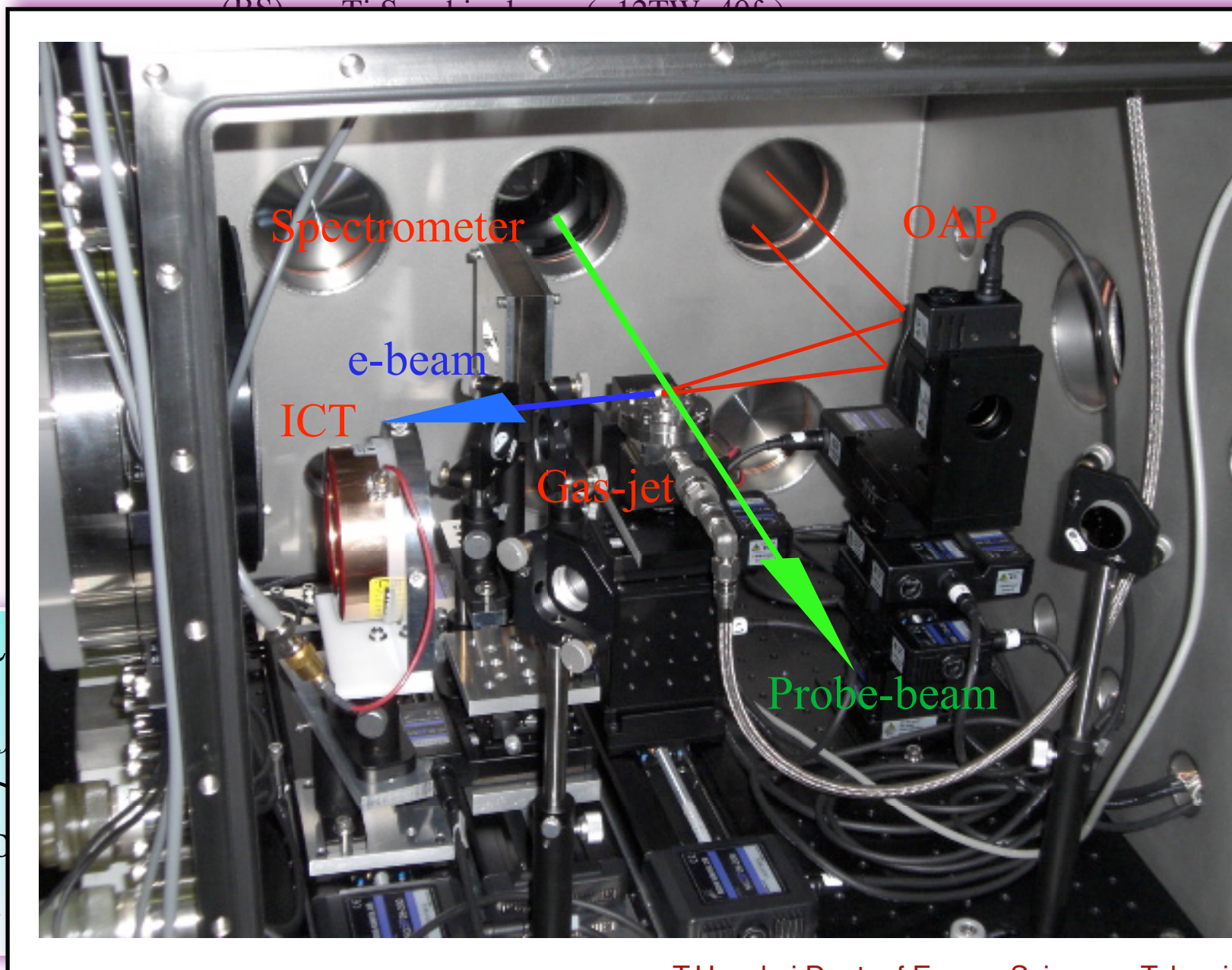
Axial B-field $\sim 0.20 \text{ T}$



Repeatable LWFA with external B-field



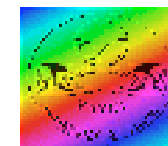
T.Hosokai, et al., Phys Rev.Lett. 97, 075004 (2006)



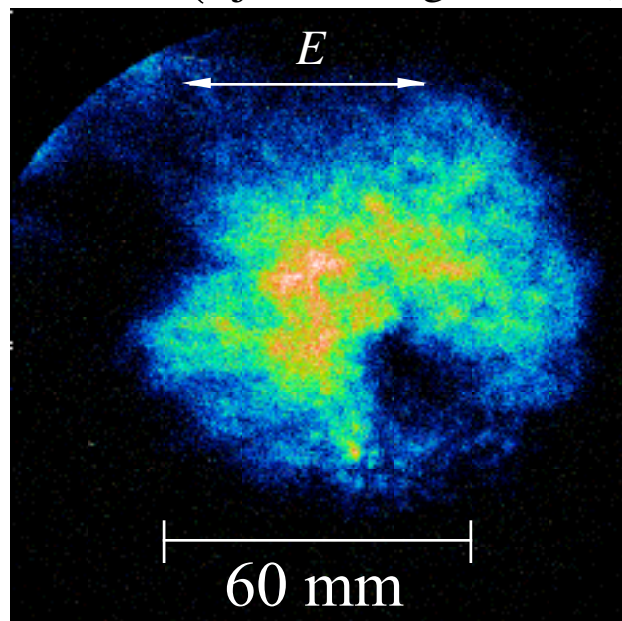
He Gas \sim
 $F^\# = 3.5$ (\sim
Laser 6 \sim
Focal spot
Rayleigh



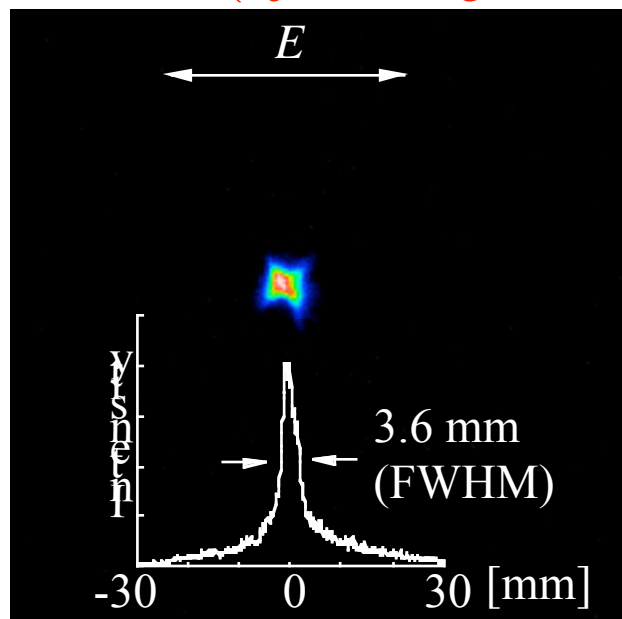
Repeatable e-Beam profiles (@ 300mm from focus point)



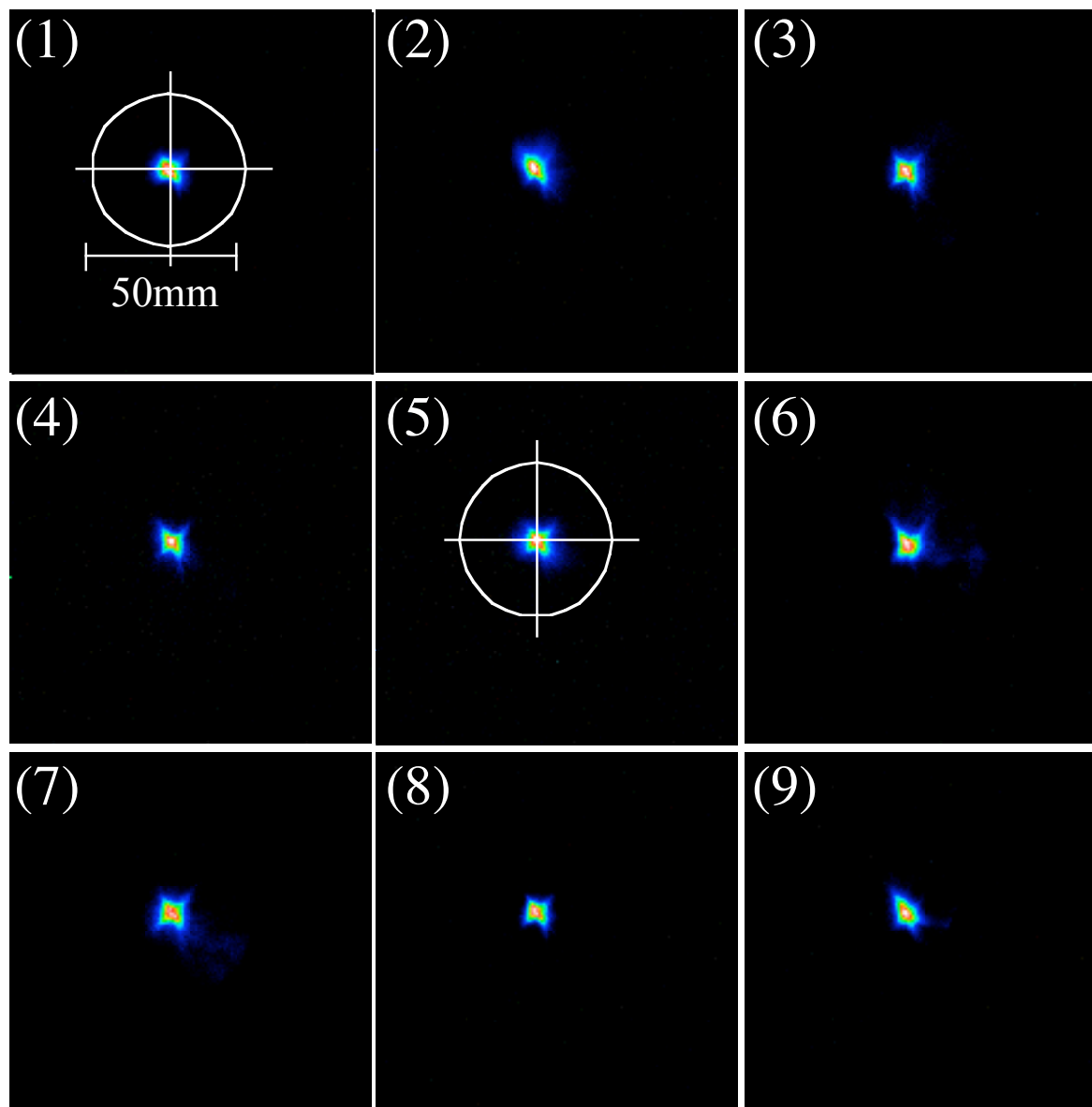
B = 0 (Ejection angle $\sim 10^\circ$)



B = 0.2T (Ejection angle $\sim 0.6^\circ$)



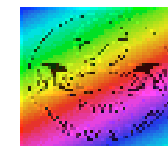
9 successive shots



(Transverse geometrical emittance $\sim 0.02\pi$ mm mrad)

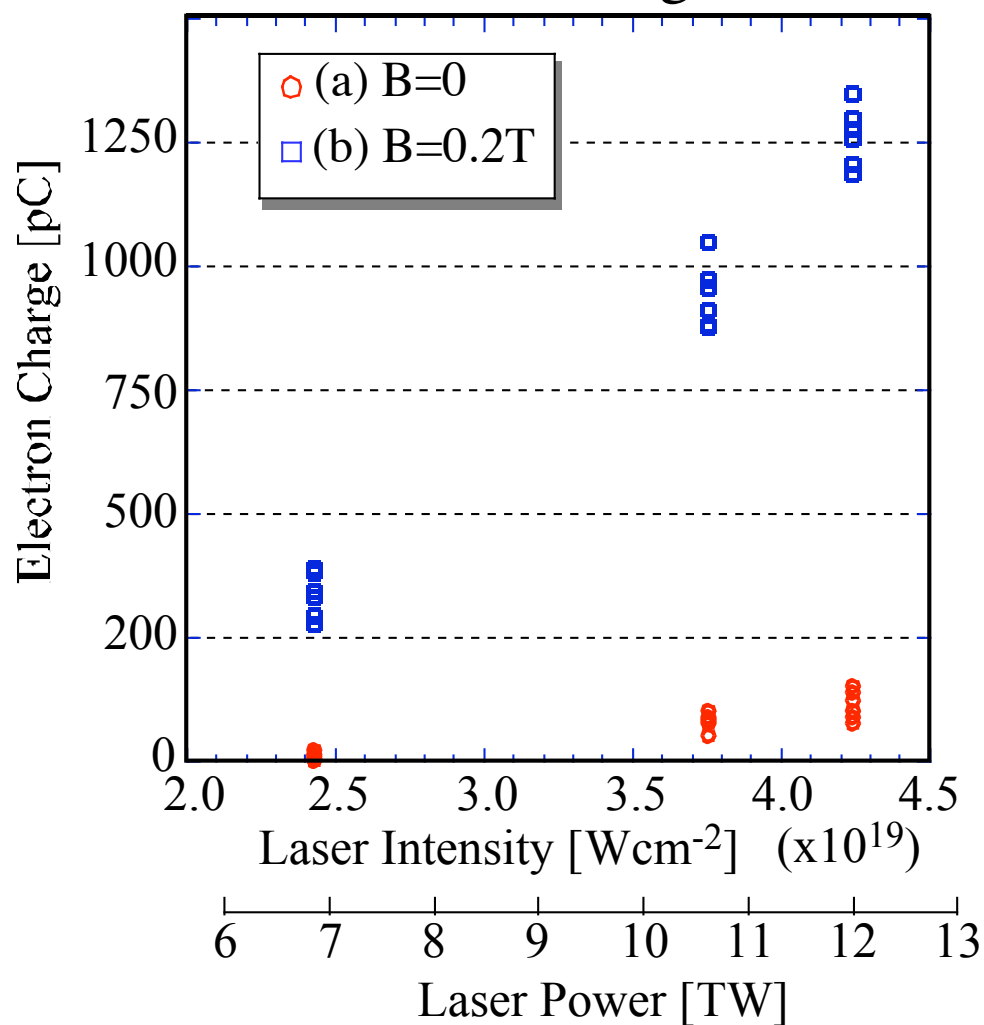


Enhanced e-Beam parameters

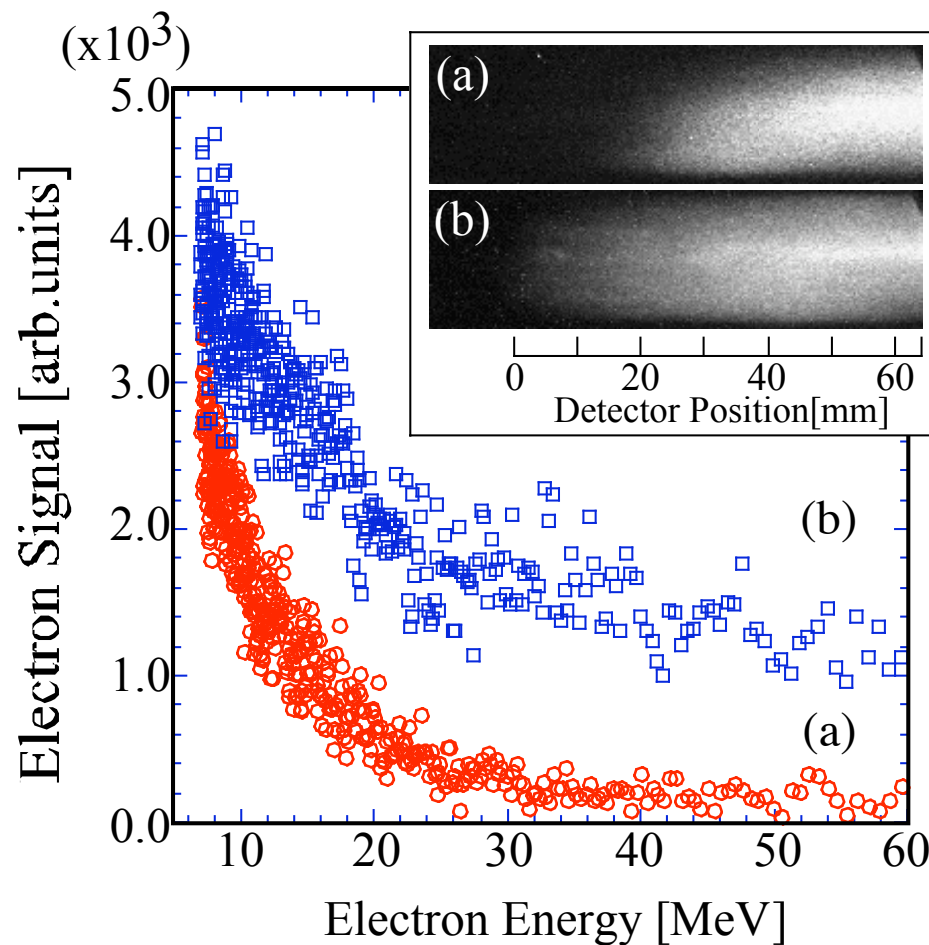


Beam size $\sim \times 1/20$
Total charge $\sim \times 10$
Charge density $\sim \times 200$

Total Charge



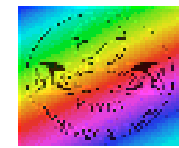
Energy Spectra



$T_h \sim 25\text{MeV}$



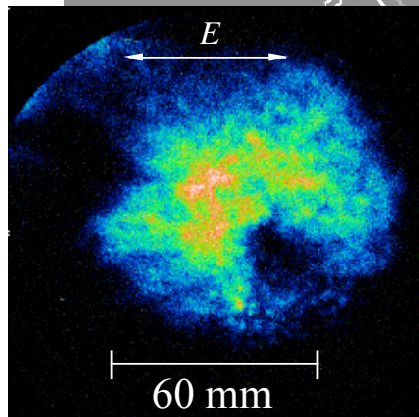
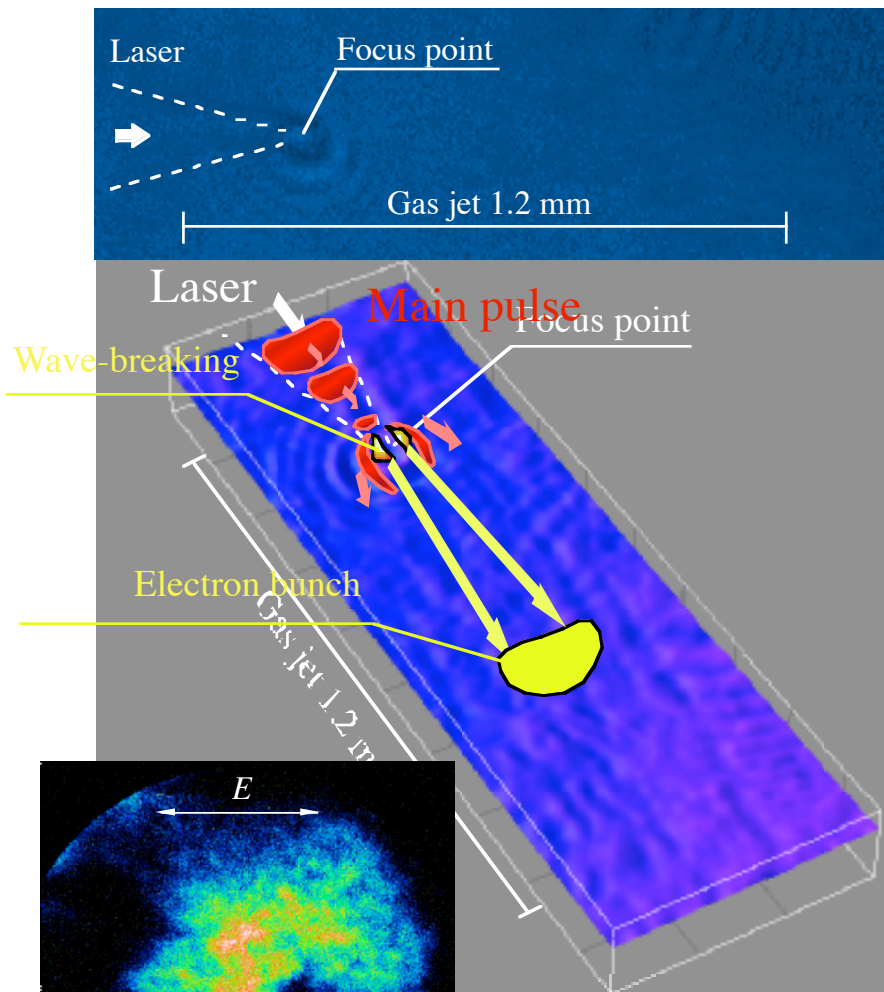
Formation of transient plasma micro-optics (TPMO) TPMO suppress laser diffraction



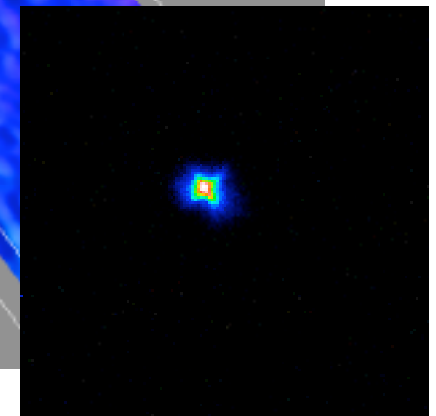
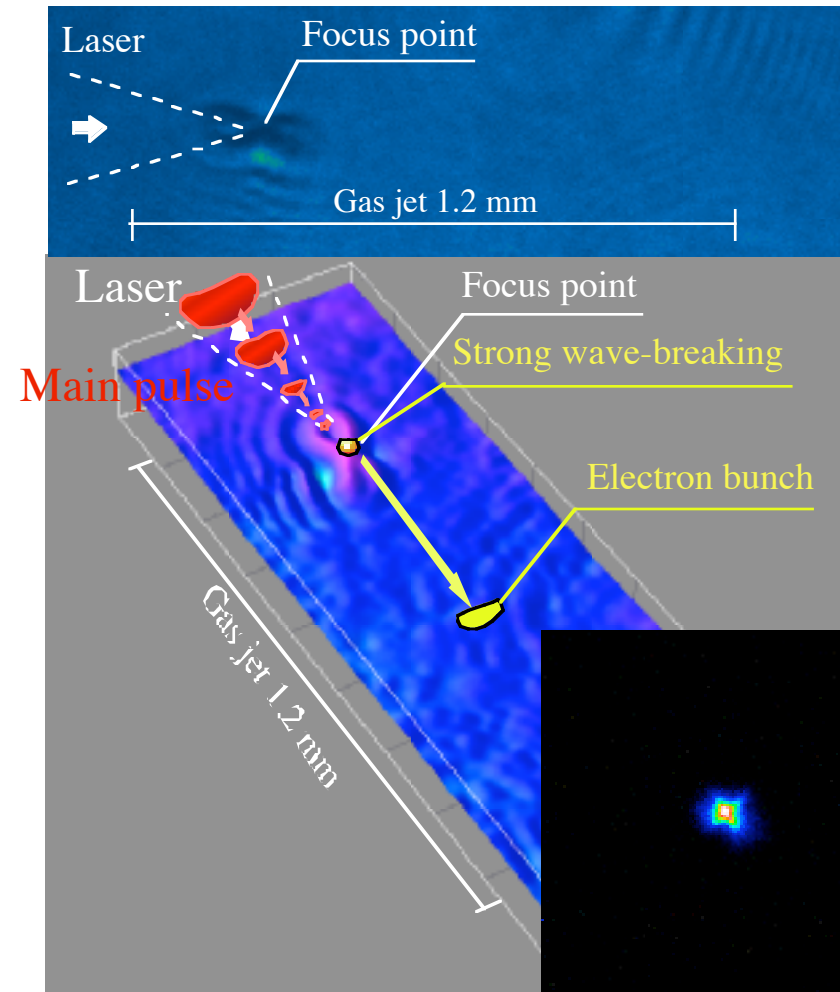
T.Hosokai, et al., Phys Rev.Lett. Submitted (Aug. 2008)

$B=0$ 1.2ps before main pulse

$B=0.2T$



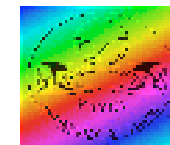
Shadowgraph image



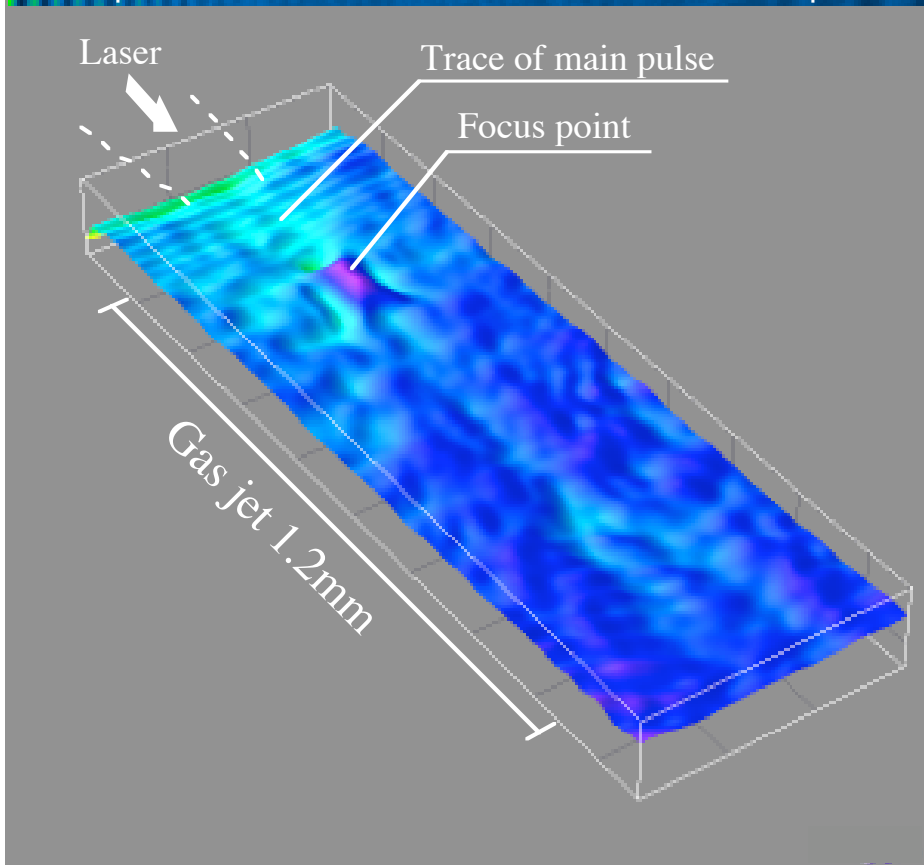
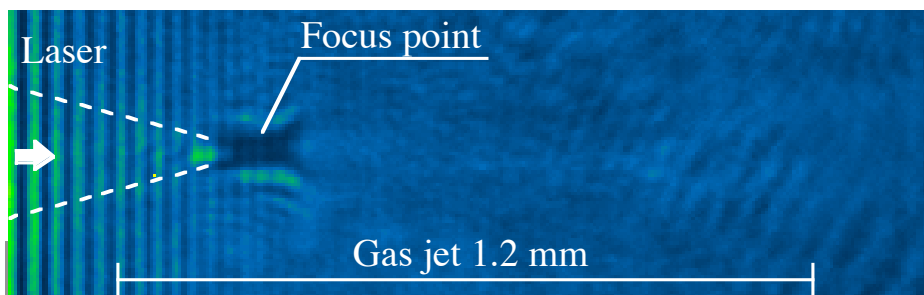
T.Hosokai, et al., Phys Rev.Lett. 97, 075004 (2006)



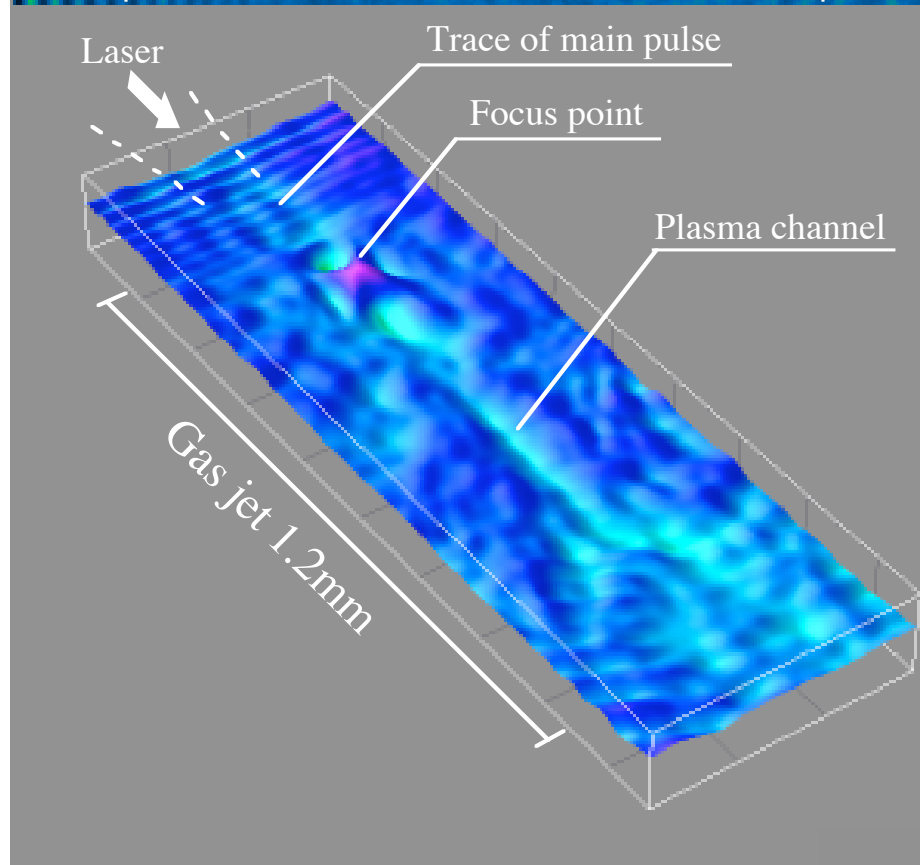
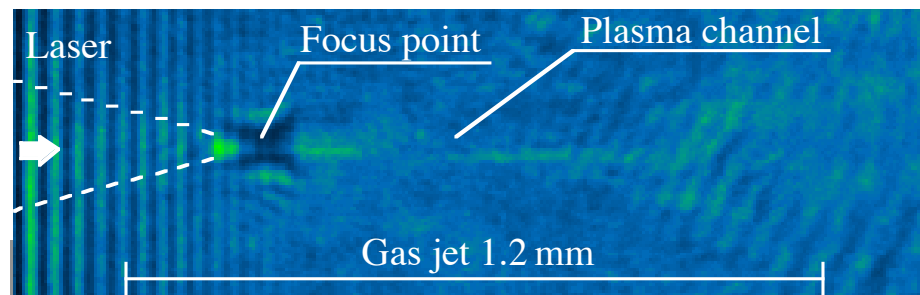
Stronger B-field experiment (1.2 mm gas-jet) with channel formation by ps pre-pulse tuning



Pre-pulse case (a), $B=1T$



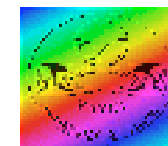
Pre-pulse case (b), $B=1T$



1.2ps before main pulse

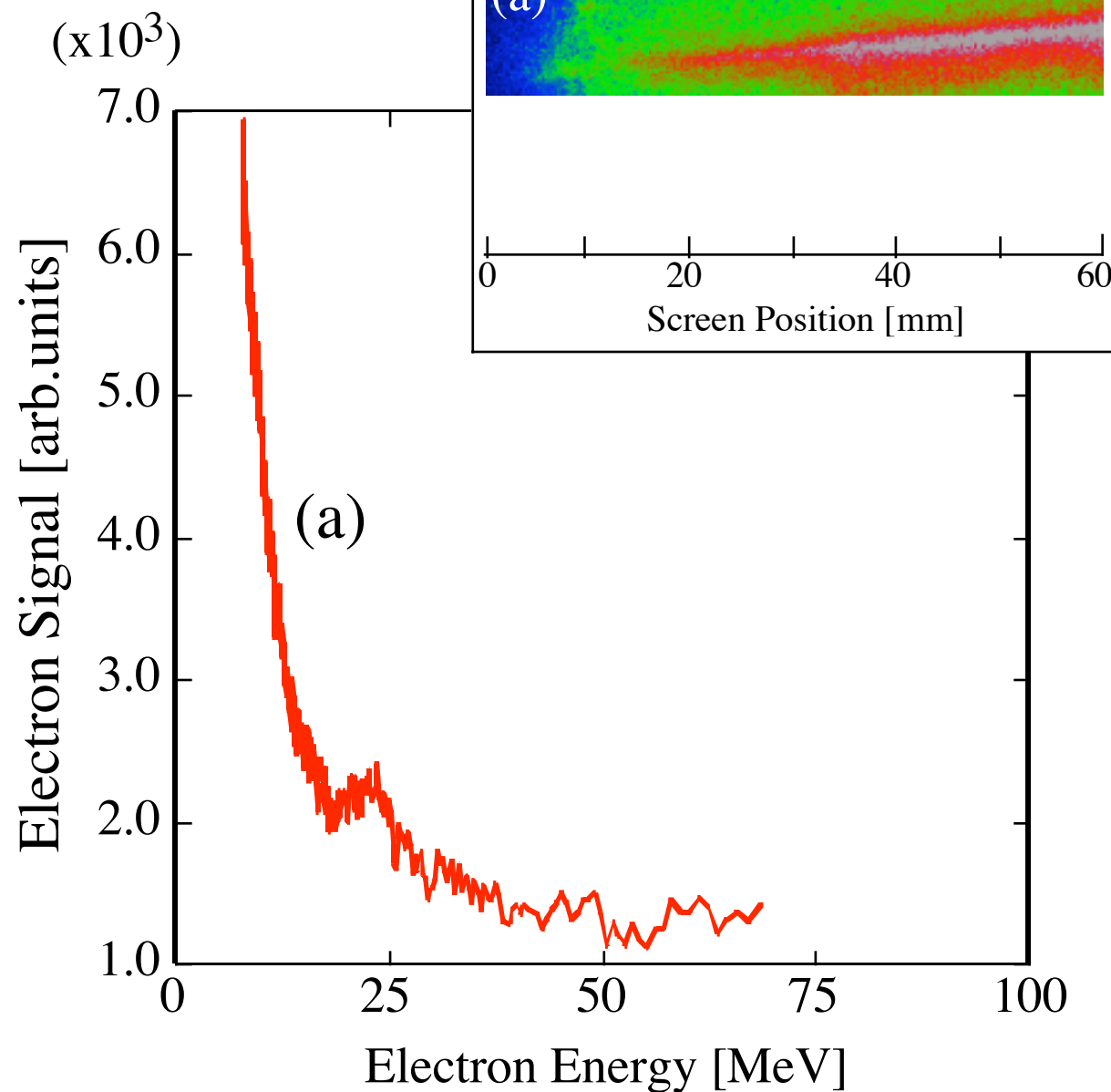
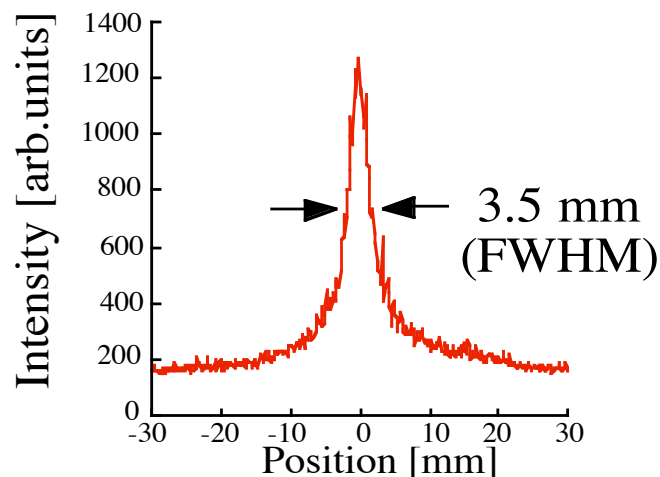
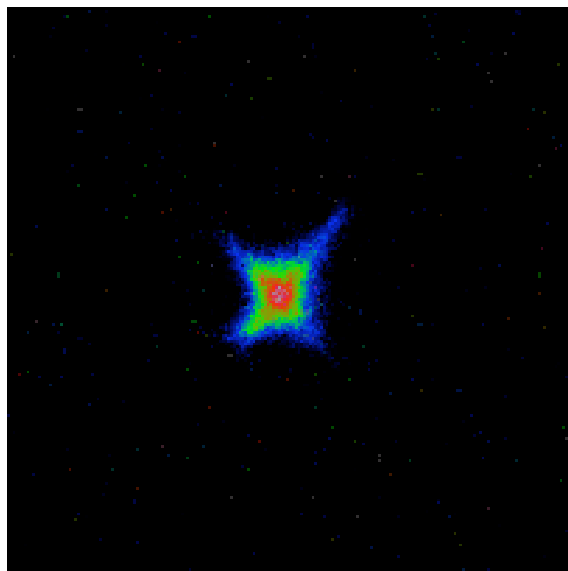


1.2 mm gas-jet experiment (e-Spot & energy spectra) Demonstration of 2-staged acceleration



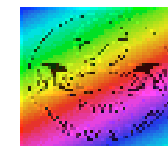
T.Hosokai, et al., Phys Rev.Lett. Submitted (Aug. 2008)

Typical electron spot image
(300 mm from focal point)



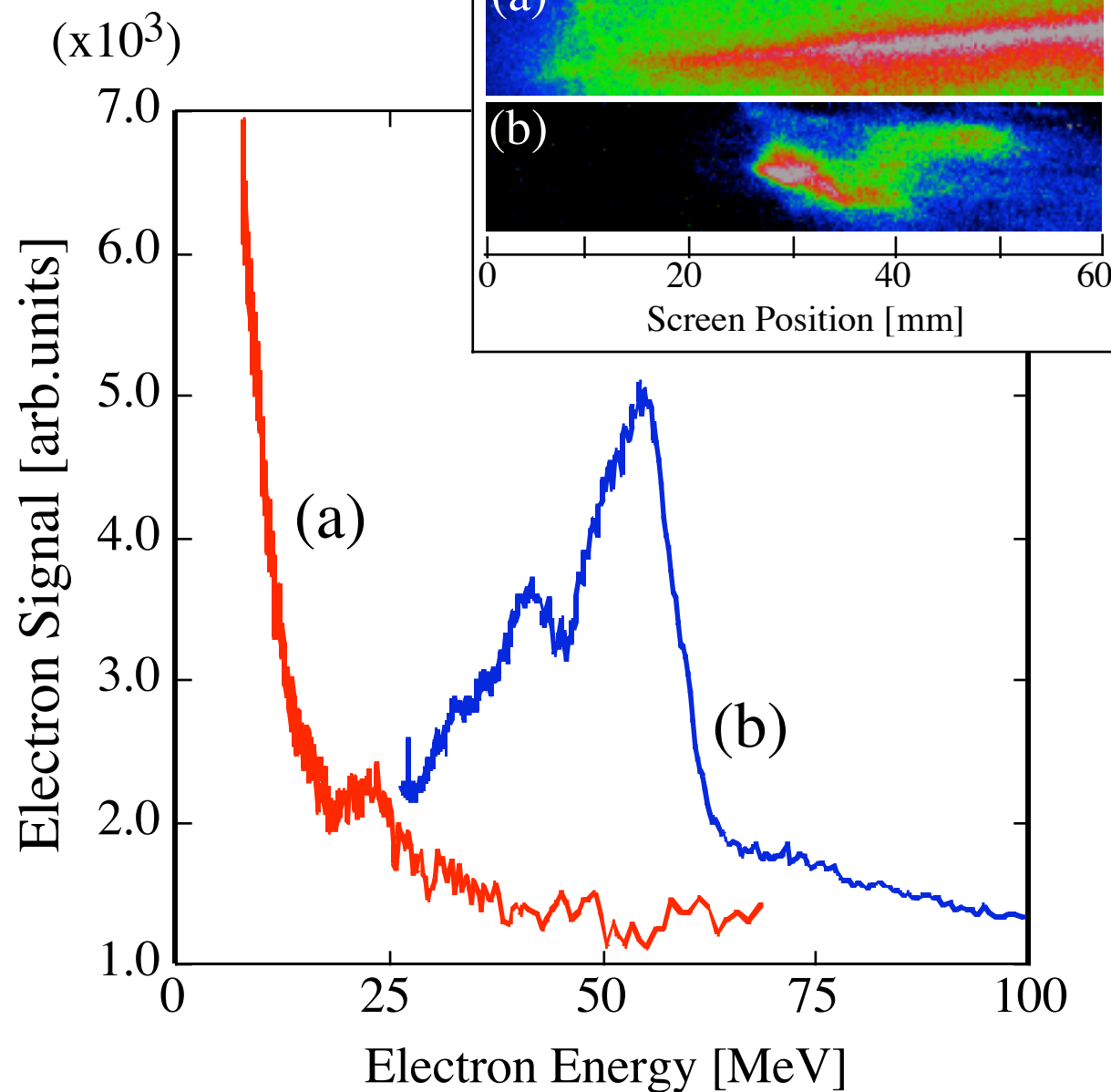
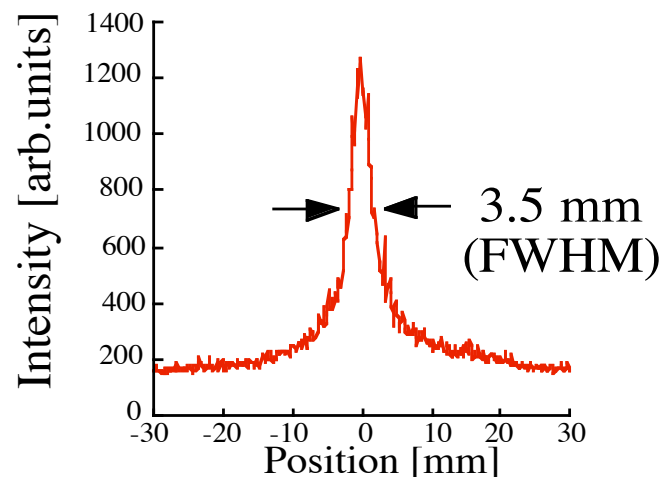
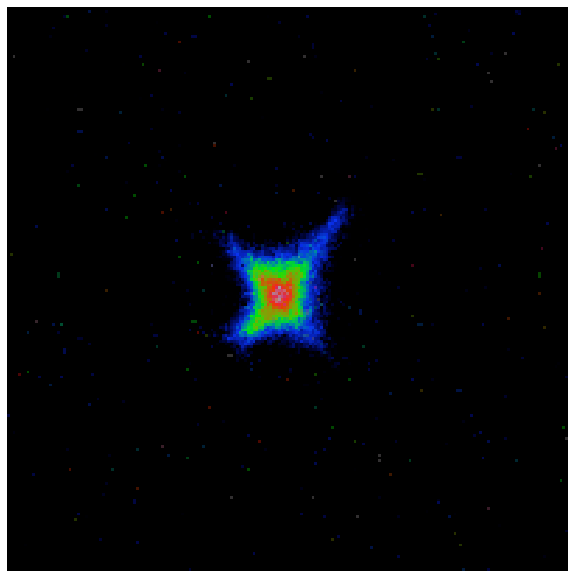


1.2 mm gas-jet experiment (e-Spot & energy spectra) Demonstration of 2-staged acceleration



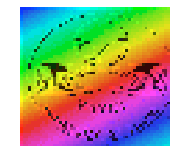
T.Hosokai, et al., Phys Rev. Lett. Submitted (Aug. 2008)

Typical electron spot image
(300 mm from focal point)

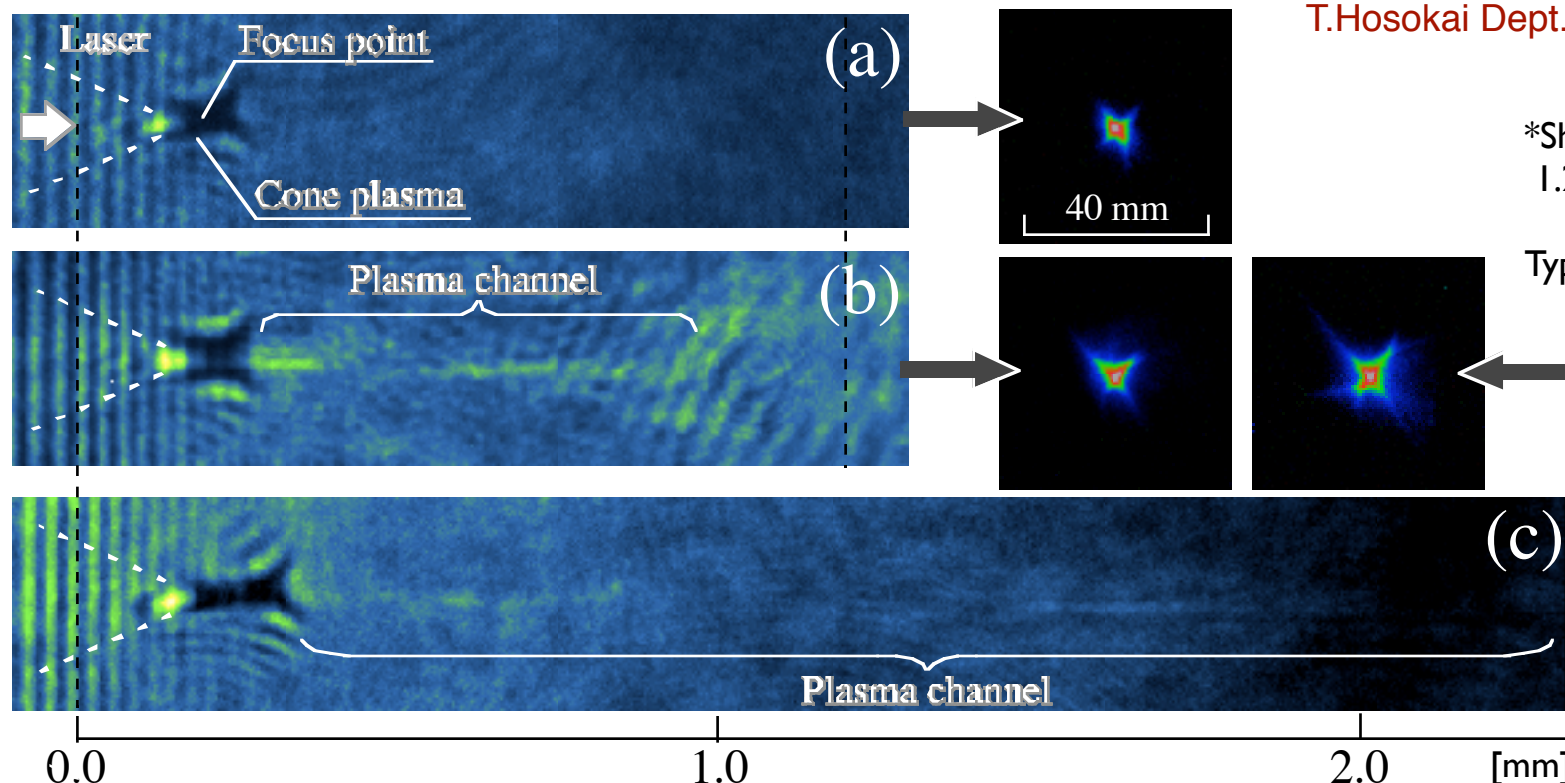




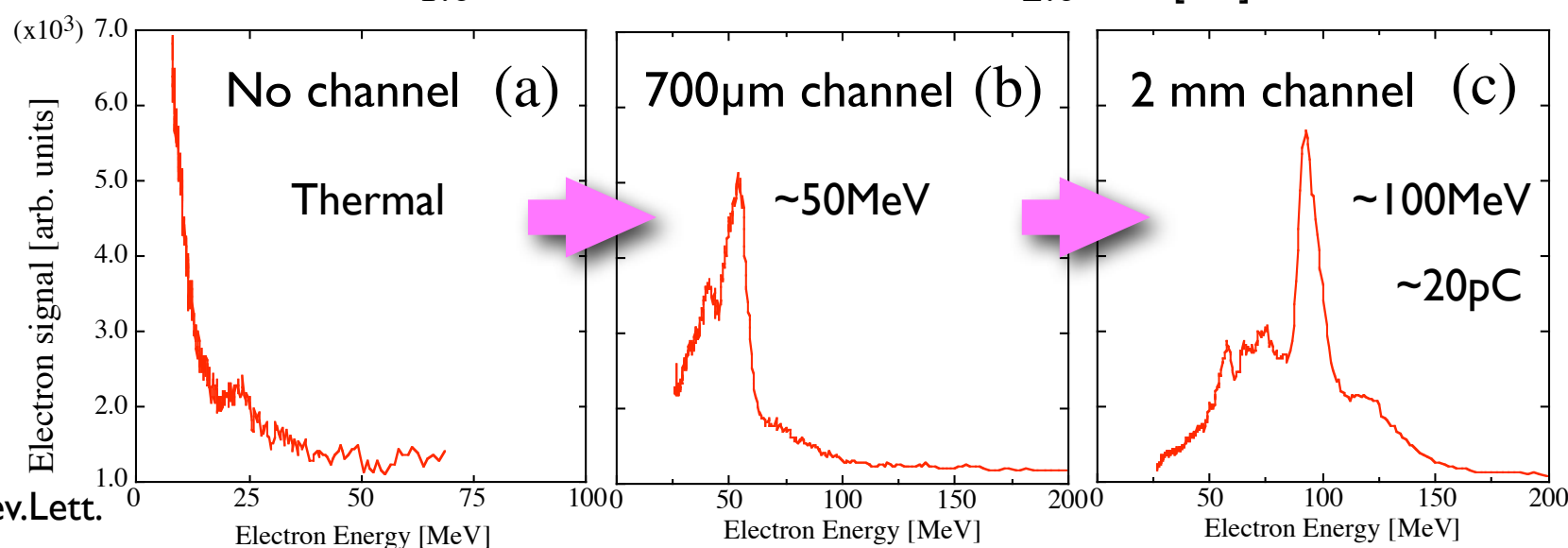
4.0 mm gas-jet experiment (e-Spot & energy spectra) Demonstration of 2-staged acceleration



T.Hosokai Dept. of Energy Sciences,
Tokyo inst. of Tech.

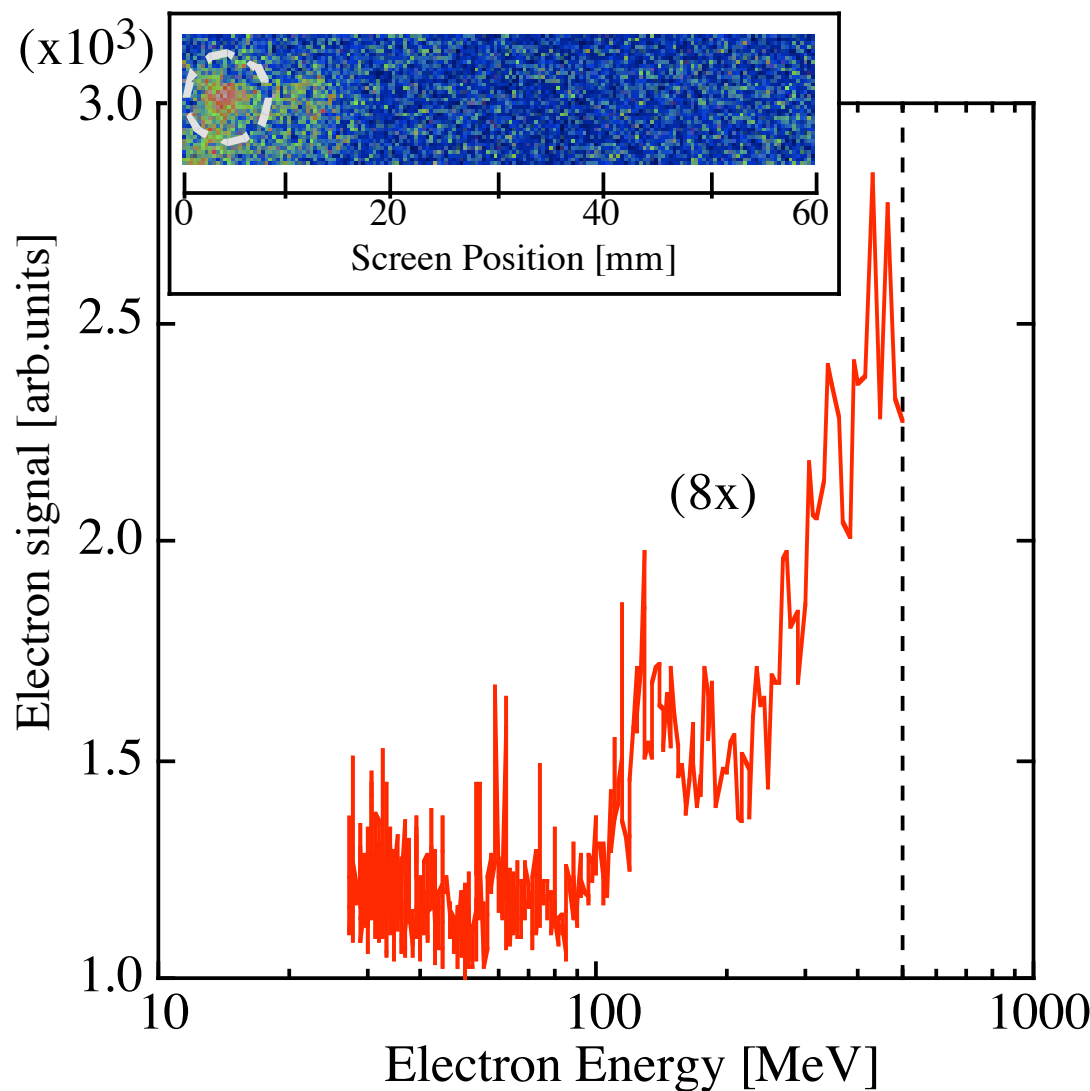
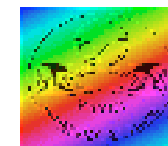


Evolution of
energy spectrum
(Staged Acc.)





Highest energy electrons measured



Single-shot measurement

Peak energy $\sim 0.45 \text{ GeV}$
(Detection limit)
 $\sim 1 \text{ pC/shot}$
 0.02 mm mmrad

Drive laser only $\sim 7 \text{ TW}$
Prepulse (b)
4.0 mm nozzle (He)
Gas density $\sim 4 \times 10^{19} \text{ cm}^{-3}$

Summary

- ☑ Table-top MeV-class Compton x-ray source can be possible by using the LWFA.
- ☑ Present problems of the LWFA is the stability of the output beam.
- ☑ Electron injection as well as capillary formation in the B-field are effective.